

DC-compliant small-signal macromodels of non-linear circuit blocks

Original

DC-compliant small-signal macromodels of non-linear circuit blocks / Olivadese, SALVATORE BERNARDO; Brenner, P.; GRIVET TALOCIA, Stefano. - STAMPA. - (2013), pp. 1-4. (Intervento presentato al convegno 17th IEEE Workshop on Signal and Power Integrity (SPI), 2013 tenutosi a Paris nel 12-15 May 2013) [10.1109/SaPIW.2013.6558330].

Availability:

This version is available at: 11583/2510281 since:

Publisher:

IEEE

Published

DOI:10.1109/SaPIW.2013.6558330

Terms of use:

This article is made available under terms and conditions as specified in the corresponding bibliographic description in the repository

Publisher copyright

IEEE postprint/Author's Accepted Manuscript

©2013 IEEE. Personal use of this material is permitted. Permission from IEEE must be obtained for all other uses, in any current or future media, including reprinting/republishing this material for advertising or promotional purposes, creating new collecting works, for resale or lists, or reuse of any copyrighted component of this work in other works.

(Article begins on next page)

DC-Compliant Small-Signal Macromodels of Non-Linear Circuit Blocks

S. B. Olivadese^{*†}, P. Brenner^{*}, S. Grivet-Talocia[†]

^{*} Intel Mobile Communications

[†] Dept. Electronics and Telecommunications, Politecnico di Torino

Abstract—This paper presents a novel strategy to improve the accuracy of macromodel-based approaches for fast Signal Integrity assessment for highly integrated Radio Frequency (RF) and Analog-Mixed-Signal (AMS) Systems on Chip (SoC). Specifically, we focus on small-signal representations of non-linear circuit blocks (CB) at prescribed DC operation points, which are approximated with low-order linearized macromodels to speed up the complex transient simulations required by common Signal-Integrity (SI) and Power Integrity (PI) verifications. In this paper, we propose a simple yet effective DC point correction strategy of the low-order macromodels, which enables their safe use in complete verification testbenches by ensuring exact biasing conditions for all circuit blocks. The numerical results show the effectiveness of the proposed model enhancement methodology, both in terms of accuracy and simulation time, when applied to several test cases of practical relevance for AMS and RF simulations.

I. INTRODUCTION AND MOTIVATION

Portable devices like smartphones and tablets are the most promising market segments for the future of consumer electronics. The increasing demand for a wide-band internet connection in conjunction with traditional cellphone systems push designers to face new challenges for the realization of rather complex Radio-Frequency (RF) transceivers and RF Systems on Chip (SOC). Digital and Analog-Mixed-Signal (AMS) circuit blocks must coexist meeting the strict size constraints imposed by portable devices. In order to offer a computational power comparable to laptops and personal computers, the digital blocks must operate with multiple operation-mode dependent high frequency clocks, that may generate a significant amount of noise at all clock harmonics. This noise may couple to the sensitive analog parts via capacitive, inductive and substrate-coupling mechanisms, thus degrading the overall system performance. Of course such issues often arise only when the whole system platform is plugged together, because only then the interferences between system components become visible. Thus, a carefully conducted pre-tapeout Signal Integrity (SI) and Power Integrity (PI) analysis is of paramount importance to tackle the verification of complex workload transmit and receive scenarios. Simulation-based SI and PI verification can then avoid the extremely expensive verification of a nearly completed system.

Due to the fact that many system control loops and CB start-up/ramp-down scenarios must be verified by simulation, transient circuit simulation is the working horse for system performance verification. However, the extreme complexity of state of the art receiver or transmitter circuits, combined with

the small time stepping forced by the RF carrier frequency, make the simulation of a full transmission burst using full transistor-level models for all the involved circuit blocks practically infeasible.

Fortunately, several components in the signal processing chain, e.g., in a RF transceiver but also in the bias control circuitry, are designed to operate nearly linearly when the specified target bias conditions are applied. This fact offers the possibility to realize a huge complexity reduction and a subsequent simulation time reduction when applying Linear Transfer Function Modelling (LTFM) techniques to such design parts [1]. In essence, a set of small-signal frequency-dependent scattering parameters are extracted, and a reduced-order linear macromodel is computed using standard methods [2]. This idea motivated the development of several SI and PI analysis techniques based on Linear Transfer Function Modeling (LTFM), like the one proposed in [3]. Please refer to [4] for a more complete survey on the available methodologies.

One issue still remaining is the creation of an LTFM which can model accurately the DC operating point of the corresponding nonlinear CB. In fact, due to the intrinsic limitations of linear models, the standard methodologies do not provide accurate results at DC, since the bias information is not included in the small-signal macromodel. To overcome this issue, we propose a simple yet effective DC operation point (DC-OP) correction strategy, capable to fix accurately the DC point for LTFMs derived from the original CB's while preserving the AC model accuracy near the operating point.

This paper is organized as follows. Section II presents the issue that motivates this work; Section III introduces the DC-OP correction strategy through a simple example; the results that show the effectiveness of the proposed approach are listed in Section IV. Conclusions will be drawn in Section V.

In the following, $a(t)$ (italic) denotes time dependent vectors, A (upper case) is used for time-independent vectors and \mathbf{A} (bold upper case) for constant matrices.

II. PROBLEM STATEMENT

Non-linear and causal systems, for which the wavelength associated to the operating frequency is much larger than the circuits physical dimensions, can be modelled via finite-order

non-linear state space equations [5]

$$\dot{x}(t) = f(x(t), u(t)) \quad (1)$$

$$y(t) = g(x(t), u(t)) \quad (2)$$

where $u(t), y(t) \in \mathbb{R}^p$ denote system inputs and outputs, $x(t) \in \mathbb{R}^n$ is an internal state vector, and $\dot{x}(t) = \frac{dx(t)}{dt}$.

When (1)-(2) represent a non-linear circuit block for AMS and RF applications, like LNA's (Low Noise Amplifiers), OPA's (Operational Amplifiers) and programmable active filters, a significant complexity reduction of these nonlinear state equations is possible. In fact, since these devices are designed to operate almost linearly when driven below maximum allowed input power or signal magnitude, the input, output and state vectors can be represented as a superposition of a constant DC term (U_{DC}, X_{DC}, Y_{DC}) and a small-signal time dependent term ($\tilde{u}(t), \tilde{x}(t), \tilde{y}(t)$) as

$$u(t) = U_{DC} + \tilde{u}(t), \quad (3)$$

$$x(t) = X_{DC} + \tilde{x}(t), \quad (4)$$

$$y(t) = Y_{DC} + \tilde{y}(t). \quad (5)$$

If only constant inputs are applied (DC conditions), we have

$$u(t) = U_{DC} \quad \text{and} \quad \dot{x}(t) = 0, \quad (6)$$

which applied to (1) and (2) leads to the definition of the DC operation point as the solution of

$$f(X_{DC}, U_{DC}) = 0, \quad (7)$$

$$Y_{DC} = g(X_{DC}, U_{DC}). \quad (8)$$

The triplet U_{DC}, X_{DC}, Y_{DC} is available from a direct DC simulation of the transistor-level circuit block.

Using (3)-(5) into (1)-(2) leads to

$$\dot{\tilde{x}}(t) = f(X_{DC} + \tilde{x}(t), U_{DC} + \tilde{u}(t)), \quad (9)$$

$$\tilde{y}(t) + Y_{DC} = g(X_{DC} + \tilde{x}(t), U_{DC} + \tilde{u}(t)), \quad (10)$$

which, under small-signal excitation, can be approximated by a first-order Taylor expansion of both state and output equations

$$\dot{\tilde{x}}(t) \approx \mathbf{A}\tilde{x}(t) + \mathbf{B}\tilde{u}(t), \quad (11)$$

$$\tilde{y}(t) \approx \mathbf{C}\tilde{x}(t) + \mathbf{D}\tilde{u}(t), \quad (12)$$

where $\mathbf{A} \in \mathbb{R}^{n \times n}$, $\mathbf{B} \in \mathbb{R}^{n \times p}$, $\mathbf{C} \in \mathbb{R}^{p \times n}$ and $\mathbf{D} \in \mathbb{R}^{p \times p}$ denote constant state-space matrices defining the small-signal Linear Transfer Function Model (LTFM) of the CB around the specified bias conditions, with frequency-dependent input-output response

$$\mathbf{H}(s) = \mathbf{C}(s\mathbf{I} - \mathbf{A})^{-1}\mathbf{B} + \mathbf{D}. \quad (13)$$

The elements of these state matrices are formally defined as partial derivatives of the various components of (1)-(2) evaluated at the current DC point. However, as discussed in [3], it is also possible to obtain the LTFM by first extracting a set of frequency-dependent small-signal Scattering $\mathbf{S}(j\omega)$, Admittance $\mathbf{Y}(j\omega)$ or Impedance $\mathbf{Z}(j\omega)$ parameters, in the following collectively denoted as $\mathbf{H}(j\omega)$, by exploiting

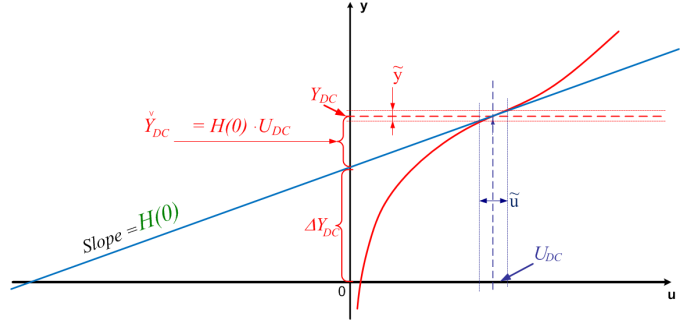


Fig. 1. Graphical illustration of the DC point correction for a static one-port case. The LTFM (blue line) provides a good (first order) approximation near the operating point of the non-linear characteristic (red curve), but the DC solution of the LTFM \tilde{Y}_{DC} from (14) has no relation with the correct DC solution Y_{DC} .

standard features of state of the art circuit solvers, namely a set of small-signal AC analyses. Then, this data is fed to a macromodeling algorithm, e.g. Vector Fitting [2], to directly obtain the reduced-order macromodel (11)-(12) by minimizing the macromodel error $\|\mathbf{H}(j\omega) - \mathbf{H}(j\omega)\|$ in the desired norm.

The LTFM usually attains a very good accuracy for the small-signal characterization of the CB in the frequency domain [3]. Unfortunately, similar good results can not be obtained from time domain (transient) simulation. In fact, a direct replacement of the nonlinear CB with the LTFM in a transient simulation setup leads to possibly incorrect biasing, since the small-signal macromodel does not include any information of the underlying DC operation point. When excited by constant inputs $u(t) = U_{DC}$, the LTFM provides its closed form DC output solution

$$\tilde{Y}_{DC} = \mathbf{H}(0)U_{DC} = (\mathbf{D} - \mathbf{C}\mathbf{A}^{-1}\mathbf{B})U_{DC}, \quad (14)$$

which has no relationship with the true DC operation point of the original CB. This information is not embedded in the LTFM, which only represents the dynamics of the small variations around the bias point. This issue is summarized graphically in Figure 1.

Considering the case of several CB's modelled as LTFM's and connected together in a long chain to realize a low complexity model of an RF transceiver path, it is clear that the DC solution of all individual simplified models must comply with the exact bias conditions, especially when some nonlinear components are still present in the testbench. An example is provided by the system level schematic of a simple receiver stage in Figure 2 [6], which shows how a circuit block driven by the outputs of the previous LTFM could receive as an input the wrong DC bias and could therefore be operating incorrectly.

III. DC CORRECTION STRATEGY

To overcome the intrinsic DC-OP accuracy limitation of the LTFM at DC, the following correction strategy can be implemented. We assume that the correct bias conditions provided by the input-output pair (U_{DC}, Y_{DC}) are known as a

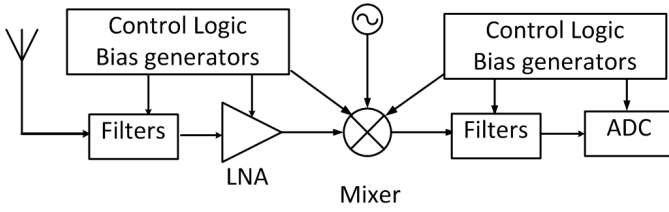


Fig. 2. Top level schematic of a basic receiver chain [6]. For the simulation of such a CB chain it is essential that each block in the chain biases the following CB correctly. Even a small error in the DC-OP modelling of some CB, like the LNA, will corrupt the performance of the following CB's.

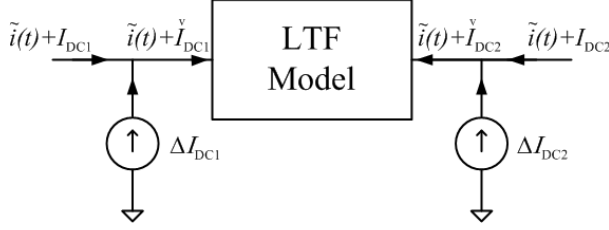


Fig. 3. DC point correction for a two port LTFM. The correct DC bias is set via constant current sources ΔI_{DC1} and ΔI_{DC2} applied at the input ports of the LTFM. The current source values are provided by the elements of the correction vector (15).

solution of (8) for the original non-linear system. Then, once the small-signal macromodel (11)-(12) is available, its closed-form DC solution \check{Y}_{DC} driven by the same nominal biasing inputs U_{DC} is computed as in (14). We then compute the difference

$$\Delta Y_{DC} = Y_{DC} - \check{Y}_{DC}, \quad (15)$$

which represents the correction that must be applied to the DC solution of the LTFM in order to obtain the nominal CB bias level.

The correction terms ΔY_{DC} are applied by defining an enlarged DC-corrected small-signal macromodel which embeds the original LTFM and adds at its interface ports suitable constant sources, whose values are the components of ΔY_{DC} . In case the k -th port input u_k is a voltage and the corresponding k -th output y_k is a current, the correction is applied as a shunt current source with value ΔY_{DCk} . Conversely, if u_k is a current and y_k is a voltage, a series constant voltage source ΔY_{DCk} is applied. The basic idea is depicted in Figure 3 for a two-port voltage-controlled device. It should be noted that using constant correction sources will affect and fix the DC point only, without any effect on the accuracy of the LTFM around the OP point under small-signal excitation.

The proposed strategy for the extraction of a low-complexity DC-compliant small-signal linear macromodel can be summarized in the following steps:

- 1) create a suitable CB characterization test bench and apply there the desired DC operation point setting to each CB pin;
- 2) extract Y_{DC} and the small-signal frequency-dependent $S(j\omega)$, $Y(j\omega)$, or $Z(j\omega)$ parameters from a circuit simulation of the non-linear system, here represented by (1)-

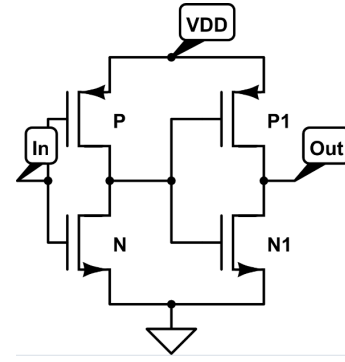


Fig. 4. A two-stage buffer.

(2);

- 3) perform a rational curve fitting of the $S(j\omega)$, $Y(j\omega)$, or $Z(j\omega)$ parameters, e.g. using VF [2], and obtain a state-space realization of the LTFM;
- 4) compute \check{Y}_{DC} from (14) and ΔY_{DC} from (15);
- 5) synthesize a circuit netlist with a standard macromodel realization, complemented by DC correction sources ΔY_{DC} at its external ports.

IV. RESULTS

This section presents some results to illustrate the effectiveness of the proposed method. The following test cases are considered.

- A two-stage buffer: this is a simple non-linear example whose netlist is depicted in Figure 4.
- A Low-Drop Out (LDO) regulator: the corresponding CB is taken from a real 3G transceiver design. This is basically a linear DC voltage regulator, controlled by external biases and a logic unit. LDO's can operate with a very small input-output differential voltage. The high level schematic of this component is depicted in Figure 5.
- A Low Noise Amplifier (LNA): the corresponding CB was also taken from a real 3G transceiver design. LNA's are widely used in receiver chains like the one depicted in Figure 2. A high level schematic for the LNA is depicted in Figure 6.

For each test case, we consider the relative error between the raw and DC-corrected LTFM responses under constant excitation by the nominal bias inputs. These errors are defined, respectively, as

$$\epsilon_{\check{y}} = \left| \frac{\check{Y}_{DC} - Y_{DC}}{Y_{DC}} \right|, \quad (16)$$

for the raw LTFM, and

$$\epsilon_{\check{y}} = \left| \frac{\bar{Y}_{DC} - Y_{DC}}{Y_{DC}} \right|. \quad (17)$$

for the DC-corrected LTFM, where \bar{Y}_{DC} represents the DC output obtained from the LTFM after the application of the DC correction sources defined by (15).

The results obtained by a circuit simulation of the original CB and synthesized LTFM are reported in Table I, where all

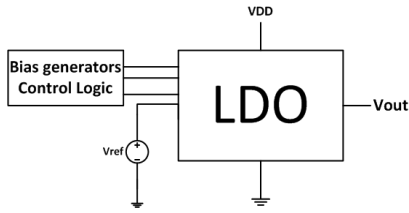


Fig. 5. High-level schematic of a Low-Drop Out (LDO) regulator CB extracted from a real transceiver block. The Control Logic can be used to select the desired voltage output V_{out} , while V_{ref} and V_{VDD} are reference and supply voltages.

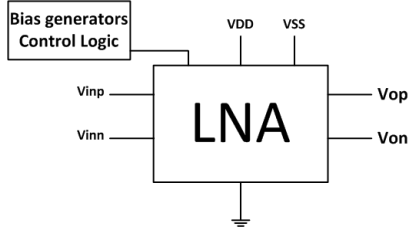


Fig. 6. High-level schematic of an integrated LNA, which is part of a real receiver chain (Figure 2); terminals V_{inp} and V_{inn} define the differential input, while V_{DD} is the supply voltage and V_{op} V_{on} define the differential output pair.

DC results for all port variables are reported, together with the corresponding LTFM relative errors. We see from this table that the DC-corrected LTFM results are exact, as expected, whereas the raw LTFM provides an incorrect DC solution.

In order to further illustrate the advantages of the proposed reduced-order modelling strategy, we performed a transient simulation of the LNA structure using both the original nonlinear CB and the small-signal raw and DC-corrected macromodels. The results are depicted in Fig. 7. We see that the DC-corrected macromodel provides practically coincident results with the reference, whereas the raw LTFM results in a DC shift of its response. We remark that the reference simulation took 10 minutes to perform a transient analysis of 500ns, whereas the DC-corrected LTFM simulation only

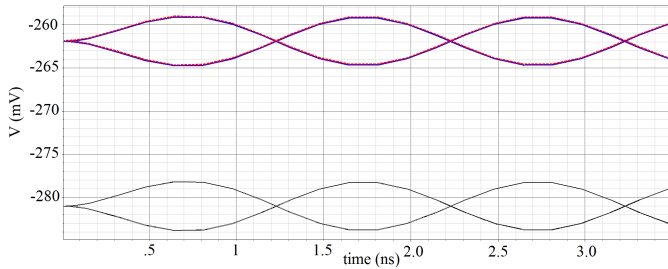


Fig. 7. Output transient results for the LNA example obtained with the original CB (solid blue line) the raw LTFM (solid black line), and the DC-corrected LTFM (dashed red line). The input signal for the LNA is a simple sine wave having 1mV peak to peak amplitude. This simple example clearly demonstrates the effectiveness of the proposed strategy. The transient response obtained using the LTFM (black solid line), is very accurate except for the vertical shift due to its incorrect DC level. The DC-corrected LTFM is completely overlapped to the transient response obtained from the nonlinear CB.

TABLE I

VOLTAGE AND CURRENTS FOR THE TEST CASES IN FIGURE 4-6. WHERE Y ARE THE DC DATA FROM THE CB UNDER ANALYSIS, \hat{Y} ARE THE DC DATA OBTAINED FROM THE LTFM BEFORE THE APPLICATION OF THE CORRECTION STRATEGY AND \tilde{Y} ARE THE SAME DATA AFTER THE APPLICATION OF THE DC CORRECTION STRATEGY. ERROR NORMS $\epsilon_{\tilde{y}}$ AND $\epsilon_{\hat{y}}$ ARE DEFINED ACCORDING TO (16) AND (17).

| Test | | Y | \hat{Y} | $(\epsilon_{\hat{y}})$ | \tilde{Y} | $(\epsilon_{\tilde{y}})$ |
|--------|-----------|-----------|-----------|------------------------|-------------|--------------------------|
| Buffer | I_{in} | -1.58e-11 | 0 | (1) | -1.58e-11 | (0) |
| | I_{out} | 1.55e-3 | 3.87e-3 | (1.5) | 1.55e-3 | (0) |
| | I_{DD} | -1.55e-3 | -3.87e-3 | (1.5) | -1.55e-3 | (0) |
| | V_{out} | 1.55e-6 | 3.87e-6 | (1.5) | 1.55e-6 | (0) |
| | V_{DD} | -3.39e-4 | -1.32e-3 | (28) | -3.39e-4 | (0) |
| LDO | I_{ref} | -2.5e-3 | -2.6e-3 | (0.04) | -2.5e-3 | (0) |
| | I_{out} | 3.39e-4 | 1.32e-3 | (28) | 3.39e-4 | (0) |
| | V_{out} | 1.294 | 1.295 | (0.04) | 1.294 | (0) |
| | V_{DD} | -1.81e-3 | 8.3e-5 | (1) | -1.81e-3 | (0) |
| LNA | I_{SS} | -1.85e-3 | 0.024 | (10) | -1.85e-3 | (0) |
| | I_{op} | -5.24e-3 | -5.62e-3 | (7e-2) | -5.24e-3 | (0) |
| | I_{on} | -5.24e-3 | -5.62e-3 | (7.2e-2) | -5.24e-3 | (0) |
| | V_{op} | -0.262 | -0.28 | (6.8e-2) | -0.262 | (0) |
| | V_{on} | -0.262 | -0.28 | (6.8e-2) | -0.262 | (0) |
| | V_{DD} | -1.81e-3 | 8.3e-5 | (1) | -1.81e-3 | (0) |
| | V_{SS} | -1.85e-3 | 0.024 | (10) | -1.85e-3 | (0) |

required 5 seconds, with a significant speedup.

V. CONCLUSIONS

We presented a simple but general strategy for the correction of the DC Operating Point of Linear Transfer Function Models (LTFM's) derived from non-linear circuit blocks. The basic idea relies on the usage of constant sources of suitable value that, applied to the input ports of the LTFM, can correct the bias point in a simple and reliable way.

The main drawback of proposed strategy is that the DC correction is only valid for a fixed DC bias point. Work is under way to parametrize both the DC correction sources and the small-signal macromodels, so that a unique DC-compliant parametrized macromodel will be available for automated system verification, as required by industrial flows.

REFERENCES

- [1] P. Brenner and U. Knöchel, "Methodology and Tools for Simulation-Based Crosstalk Analysis in RF and Mixed Signal SoC's and SiP's", edaWorkshop, Tagungsband, Hannover, May 2010.
- [2] B. Gustavsen, A. Semlyen, "Rational approximation of frequency domain responses by vector fitting", *IEEE Trans. Power Del.*, vol. 14, no. 3, pp. 1052-1061, Jul. 1999.
- [3] S. Grivet-Talocia, P. Brenner, F.G. Canavero, "Fast Macromodel-based Signal Integrity Assessment for RF and Mixed-Signal Modules", *IEEE International Symposium on Electromagnetic Compatibility 2007*, pp.1-6, 9-13 July 2007.
- [4] M.H. Zaki, S. Tahar, G. Bois, "Formal Verification of Analog and Mixed Signal designs: A survey", *Microelectronics Journal*, vol. 39 pp. 1395-1404, Elsevier 2008.
- [5] L.O. Chua, C.A. Desoer, E. S. Kuh, "Linear And Non Linear Circuits", McGraw-Hill 1987.
- [6] R. Behzad, *RF microelectronics*, Prentice Hall 1998.